ELSEVIER

Large hydrocarbon fuel pool fires: Physical characteristics and thermal emission variations with height

Phani K. Raj *

Technology & Management Systems Inc., 102 Drake Road, Burlington, MA 01803, USA

Abstract

In a recent paper [P.K. Raj, Large LNG fire thermal radiation-modeling issues and hazard criteria revisited, Process Safety Progr., 24 (3) (2005)] it was shown that large, turbulent fires on hydrocarbon liquid pools display several characteristics including, pulsating burning, production of smoke, and reduced thermal radiation, with increasing size. In this paper, a semi-empirical mathematical model is proposed which considers several of these important fire characteristics. Also included in this paper are the experimental results for the variation of the fire radiance from bottom to top of the fire (and their statistical distribution) from the largest land spill LNG pool fire test conducted to date.

The purpose of the model described in this paper is to predict the variation of thermal radiation output along the fire plume and to estimate the overall thermal emission from the fire as a function its size taking into consideration the smoke effects. The model utilizes experimentally measured data for different parameters and uses correlations developed from laboratory and field tests with different fuels. The fire dynamics and combustion of the fuel are modeled using known entrainment and combustion efficiency parameter values. The mean emissive power data from field tests are compared with model predictions. Model results for the average emissive powers of large, hypothetical LNG fires are indicated.
© 2006 Elsevier B.V. All rights reserved.

Keywords: Smoke; LNG fire; Emissive power; Thermal radiation; Liquid fuel; Pool fire

1. Introduction

It is known from field experiments conducted with different liquid fuels that the burning characteristics and the physical behavior of pool fire changes as the size (diameter) of the fires increases (AGA [3], Raj et al. [8], Malvos and Raj [14], Mizner and Eyre [16]). Therefore, extrapolation of the results (especially thermal radiation emissions) from small-scale experiments for predicting the characteristics of large size fires occurring in postulated accidental liquid fuel release scenarios (from terminal storage tanks, ships, barges and other large volume transports) is prone to significant errors unless a detailed turbulent diffusion fire model with proper combustion chemistry is used. Unfortunately, the current generation of models used by the scientific community and regulatory agencies in the US, for predicting hazard zones surrounding postulated large pool fires of liquefied natural gas (LNG) caused by large scale releases suffer from

this problem (i.e., small scale experimental results are used, erroneously, for predicting large size fire effects). The result is the prediction of overly conservative and alarmingly large hazard zones, which, needless to say, disturbs the public at large.

Attempts are being made in several research institutions to use Computational Fluid Dynamic (CFD) codes to model large diffusion fires. The degree of success in these investigations is reported to be limited in both accuracy of predictions and economics of computational resources. A discussion of the state-of-the-art related to the use of CFD codes to predicting turbulent diffusion fires is indicated in a recent paper, Raj [1]. The current state of the art is not close to having a universally applicable and economically useable model whose results agree with all data (physical characteristics and radiative output of liquid pool diffusion fires) from field tests. Hence, at least for the near future, semi-empirical models, based on the best available experimental data from as large a scale as has been tested to date must suffice. This paper proposes such a semi-empirical model, which takes into account the description of the physical fire characteristics, overall combustion chemistry, variation of the thermal output from different parts of a large turbulent diffusion fire, and

* Tel.: +1 781 229 6119.
  E-mail address: tmsinc1981@verizon.net.

Nomenclature

A	a fuel property and dynamics dependent constant
C_a	specific heat of air (assumed the same for all gases) (J/kg K)
C_S	concentration of smoke particles in the fire (kg/m^3)
D	diameter of the base of the fire (or liquid pool diameter) (m)
D_{Opt}	optical path length consistent with the type of fuel burning (m)
D	Damkohler number $= \Delta H_c/(C_a T_a)$
$E(Z)$	emissive power of the fire nominal surface at axial position Z (kW/m^2)
E_b	emissive power of the fire nominal surface near the base (kW/m^2)
E_{max}	blackbody emissive power at the base flame temperature (kW/m^2)
E_S	emissive power of the fire nominal surface covered by smoke (kW/m^2)
F_c	combustion Froude number $= (\dot{m}''_f/\rho_a\sqrt{gD})$
g	acceleration due to gravity (m/s^2)
ΔH_c	heat of combustion of the fuel (J/kg)
k_m	specific soot extinction area (m^2/kg)
L	length (height) of the visible fire plume (m)
L_C	length (height) of the bottom "clean burning zone" (m)
L_F	mean length (height) of the visible fire plume (m)
L_I	length (height) of the intermittency zone (m)
$\dot{m}(Z)$	total mass flow rate of gases at any height Z (kg/s)
$\dot{m}_a(Z)$	mass rate of entrainment of air up to height Z (kg/s)
$\dot{m}_f(Z)$	mass rate of fuel burning up to height Z (kg/s)
$\dot{m}_{f,0}$	mass rate of fuel feed into the fire at the base (kg/s)
$\dot{m}''_f$	mass flux of fuel vapor at the base of fire $(kg/s\,m^2)$
p	probability at height Z of finding, at any time, on the surface of the nominal cylinder the emission from the inner core flame unobscured by smoke
$\dot{Q}(Z)$	heat produced by combustion of fuel up to height Z (W)
r	air to fuel mass ratio for stoichiometric combustion
$T(Z)$	mean temperature of the gases at any height Z (K)
T_a	air temperature (K)
U_{wind}	wind speed (m/s)
U^*	dimensionless wind speed
$U(Z)$	cross-sectional average upward velocity of gases at any height Z (m/s)
$\bar{U}(Z)$	vertical height averaged upward gas velocity up to height Z (m/s)

Greek symbols

α	air entrainment coefficient
β	mass fraction of air that is entrained up to any height Z that burns stoichiometrically with fuel
ρ	density of gases (kg/m^3)
ρ_a	density of air (kg/m^3)
τ_s	transmissivity of smoke
ψ	ratio of "clean burn zone" axial length to mean fire plume length L_C/L_F

Subscripts

a	air
c	combustion condition
f	fuel vapors
0	fire base condition

predicts the total thermal energy radiated from the fire. Available data from large LNG fire tests (The Montoir, 35 m diameter tests) are reviewed and the model predictions are compared with measured data for thermal emission. Smoke formation in large liquid fuel fires and its effect in obscuring the thermal radiation from different parts of the fire are considered in the model described below.

The earliest models to predict the extent of the thermal hazard zone arising from the radiative emissions from a LNG pool fire were proposed in 1970s, May and McQueen [2], AGA [3], Raj and Kalelkar [4], Raj and Atallah [5] and Raj [6]. May and McQueen model considered the fire as a point source, with a constant fraction of combustion energy being released as thermal radiation and calculated the radial distance to a specified level of thermal flux hazard using the inverse square law. Other models considered the time averaged visible fire plume to be represented by an enveloping right circular cylinder (of base diameter equal to the liquid pool diameter) under calm conditions, and a tilted plume under windy conditions, with circular horizontal cross-sections. The cylinder was assumed to be a grey body of uniform emissive power (and, therefore, of a specific equivalent black body temperature and constant emissivity) over the entire cylinder surface, the emissive power itself being "back calculated" from experimental data. The LNG fire emissive powers thus calculated have ranged from $100\,kW/m^2$ (for a 1.8 m diameter fire, AGA [3]) to $275\,kW/m^2$ (for a 35 m diameter fire, Nedelka et al. [15])[1] showing the general trend of higher emissive power with increase in fire diameter. The only difference in the models applicable to a LNG fire on water and that on land was the variation in the liquid evaporation rate (spill on water resulting in a higher evaporation rate and, hence, a higher combustion rate) and its effect on the fire plume size. The emissive power for equivalent diameter fires was the same irrespective of the substrate.

---

[1] It should be noted that there are differences in how the emissive power value calculated from experimental data is reported. It can vary from a value calculated from wide angle radiometer readings and the actually photographed fire emission surface areas to that corrected for the atmospheric absorption and based on the nominal fire area determined by the equivalent right cylinder of height given by a correlation. Using the latter approach the emissive power for the Montoir 35 m diameter fire changes from $275\,kW/m^2$ to $175\,kW/m^2$.

Moorhouse [7] has taken into account the phenomenon of wind induced vapor drag on the ground (for land spill fires) resulting in the extension of the firebase in the downwind direction. This drag induced physical shape change was assumed to persist all the way to the top of the plume. The result of this assumption is to make the plume cross-section elliptical, with the major axis aligned in the wind direction. Raj et al. [8], and Considine [9] consider the LNG fire emission to come from both gaseous band emissions and continuous emission from luminous soot and provide approaches to calculate the grey body emissivity as a function of fire size. A good discussion of the current models by which the radiant heat hazards from hydrocarbon liquid fuel fires are calculated, without considering the details of smoke obscuration effect, is given by Beyler [10]. In a more recent paper Raj [11] has shown the detailed spectral emission signature of 13 m diameter LNG fire and discussed how the spectral data can be used to predict the fire thermal emission magnitude. None of the above referenced models have considered the pulsating behavior of large fires nor have they considered the formation of dark smoke and its effects in reducing thermal radiation emission from large LNG fires.

Considine [9] in his review alludes to a model by Smith [12], which includes the effect of smoke obscuration in the upper regions of fire. The radiation from the upper regions is modeled by defining a mean radiating edge together with an associated mean radiation temperature (T_R) for the upper parts of a fire. The temperature at the fire surface is assumed to vary as the square of the sine of time with an effective period of about 1 s. The amplitude of temperature variation in the smoky region of the fire is assumed to be about a 30% of the "surface" temperature in the lower regions of the fire (without smoke effects). It is concluded in this model that the upper regions of the fire (smoky regions) radiate with about 30% of the radiant heat flux emanating from the "lower region". Also, the lower region is assumed to extend to 30% of the average visible flame height. A similar "two-zone" model has also been proposed by McGrattan et al. [13] for large hydrocarbon fires. The lower region, termed the "luminous region" is the only radiating surface and the top (rest of fire plume) is assumed to be obscured by opaque smoke. Based on data measurements up to 20 m diameter fires of gasoline, heptane, crude oil and kerosene fires the authors conclude that the maximum height of the luminous region is a constant beyond a 20 m diameter fire and this maximum height is dependent only on the combustion heat release rate per unit area of the pool (for crude oil fire of 20 m diameter with a 2 MW/m² heat release rate the predicted height of bottom luminous zone is 12.8 m). In addition, in this model, the maximum emissive power of the "luminous" part of the fire does not exceed 100 kW/m².

The LNG fire thermal emission magnitude data and its variation with height obtained from the 35 m diameter LNG fire tests at Montoir (Malvos and Raj [14]) indicate that neither the Considine model nor the McGrattan et al., model predicts the fire physical characteristics and the radiation emission properly. The data indicate that the extent along the plume of the lower, "constant emissive power" region is about 6–7% of the overall mean
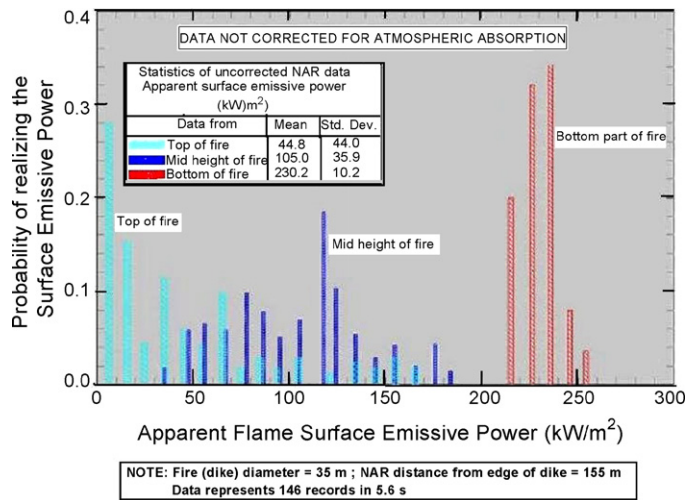
Fig. 1. Narrow angle radiometer readings from the firebase, mid height and top of a 35 m LNG pool fire in insulated concrete dike in test 2.

visible plume length (75 m). That is, the region is only about 5 m in height, whereas, the Considine model predicts this region to be 30% of 75 = 22.5 m in axial length, and the McGrattan et al., model predicts this region to be 45 m in height! The experimental data also indicate that the radiation emission varies considerably with height, decreasing almost linearly with distance along the plume axis. Fig. 1 shows the measured narrow angle radiometer data together with its statistical variation (due to the effects of turbulence, smoke obscuration effects and intermittency in the visibility of the gas burning inner zone—detailed discussions on these phenomena are provided in Section 6)[2]. The Considine model assumes a constant 30% of base emissive power for upper fire regions, whereas, the McGrattan et al. model assumes zero emission from this region. Obviously, these two models do not predict the overall emissions (and their variation with height) from large LNG fires accurately. Also, because of the two-zone, fixed emissive power (in each zone) approach the models predict higher distances for high heat flux hazard criteria (such as for exposure of objects and structures). If the overall energy radiated is the same as from a large fire (and these have been properly distributed in the two zones) then the distances calculated by these models for low heat flux exposure criteria (such as for people exposure) would be acceptable provided proper accounting is made for the atmospheric absorption of radiant heat from different parts of the fire. It should be noted that neither model takes into account the chemistry and the magnitude of soot production and their relationship with the properties of the fuel burning and fire size. A semi-empirical model that considers smoke production rate, variation of the emissive power with height, dependence on fire size and the variation with size and fuel properties of the height of the bottom "luminous" zone is presented in this paper.

---

[2] Also the variation of the mean and standard deviation of the measured emissive power along the axis of the fire plume is shown in Fig. 3 from a 35 m diameter LNG fire test.
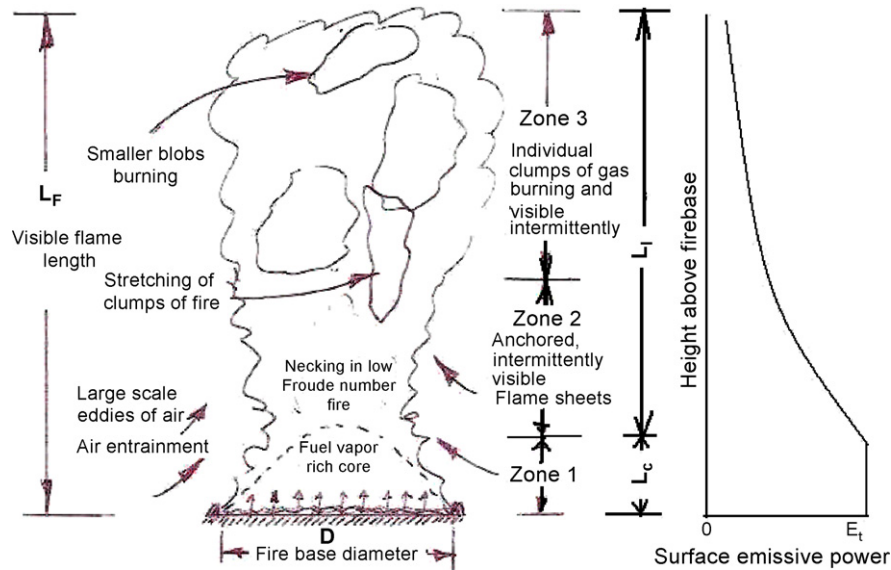
Fig. 2. Schematic representation of different regions of combustion and intermittency in a buoyant diffusion fire.

1.1. Smoke production in fires

Large diameter LNG fires seem to produce a significant amount of smoke (Nedelka et al. [15]) and is similar to those observed in the burning of other liquid fuels such as propane, butane, gasoline, kerosene (Mizner and Eyre [16]), crude oil (Notarianni et al. [17]), and JP4 (Raj [26]) of higher hydrocarbon content. Two physical phenomena may contribute to the production of smoke, even in "clean burning" fuels such as LNG. The first is the lack of enough oxygen in the core of large diameter fires to burn the carbon produced by the pyrolysis of fuel vapor. This not only produces soot (carbon particles) but also lowers the overall heat release – and hence the temperature – resulting in the promotion of smoke production. The second phenomenon may be due to the lowering of the effective concentration of fuel and vapor in the core from the recirculation of burnt gases by the toroidal vortex that is prevalent in all large fires. The effect of smoke is to shield the emission of thermal radiation from the fire thereby reducing, significantly, the thermal radiation hazard distance around large LNG or other fires. In addition, the formation (and recirculation) of smoke could result in less efficient combustion of the fuel and result in the lowering of the effective flame temperature. However, the reduction in the radiant emission out of the fire tends to increase the temperature of the gases; which one of the two effects dominates depends on the chemical properties of the fuel, chemistry of combustion, the physical dimensions and the hydrodynamics of gas flow within the fire. No model exists that considers all of these phenomena.

Soot is an agglomeration of fluffy carbon particles (with diameters in the range 3–30 nm) in a fire in which they are being oxidized and are "glowing"; in fact, the visibility of a fire is caused by the emission of radiation in the visible spectrum by the burning soot. When the carbon produced by the fuel vapor pyrolysis is either partially oxidized or is not oxidized at all because of lower local temperature, carbon particles agglomerate to form long chain molecules of carbon or "smoke". Notarianni et al. [17] measured the smoke production in crude oil fires of diameters from 0.085 m to 17.2 m and found that smoke yield (mass% of burnt fuel that is emitted as smoke) increases as the diameter of the fire increases. Soot formation studies from small, laboratory, scale tests are reported extensively in the literature (see Narasimhan and Foster [18], Hura and Glassman [19], Markstein [20], Fowler [21]). However, there is very little work on the measurement of smoke production rates in large turbulent diffusion fires and singularly absent for LNG fires. McCaffrey and Harkleroad [22] have presented soot data from laboratory-scale experiments for a number of hydrocarbon fires in the form of specific extinction area (SEA) for soot; for propane SEA is found to be 124 m²/kg and for crude oil fires it is 1000 m²/kg. No direct data for the smoke yield, as a function of fire diameter exists for large fires of different fuels. Data on smoke yield from methane (or LNG) fires are unavailable in the literature for either small scale or large scale turbulent diffusion fires! Also not available is the smoke extinction coefficient for soot formed in methane fires.

2. The model

The model discussed this paper is based on physical phenomena in a (circular geometry) turbulent diffusion fire represented schematically in Fig. 2. The buoyant plume entrains ambient air and this air is "conveyed" to different interior parts of the fire by the self-generated turbulence augmented by wind turbulence. In the bottom region of the fire, below a height L_C, combustion of the vapor is very efficient. The flame sheet visible in this region is the outer layer of vapors burning and in a large diameter fire this part of the fire is practically optically thick and radiates at a high temperature. In the region designated as zone 2, the flame sheets are anchored to the base, but represent the less efficient combustion zone in a large fire because of the mixing internally of the unburnt and partially burnt gases (due to deficiency of oxy-

gen in the central core region) from zone 1 and recirculation due to buoyant thermals. In this zone the intermittent formation of black smoke is observed which begins to partially obscure the hot interior flame. In the top region the gas burning is in clumps and generation/accumulation of significant amount of smoke is seen.

In zone 3, substantial to total shrouding of interior burning regions occurs. The result of such burning, noticed in all 'large' liquid hydrocarbon fuel fires, is a reduction of the thermal radiative output to the surroundings. This does not, however, mean that the temperature inside the fire is lower in large fires.[3] The diameter of the fire at which it can be considered to be 'large' depends upon the fuel chemical composition (especially on the carbon to hydrogen mass ratio), burning rate (dictated by feed back energy from the fire as well as heat input from the substrate) and environmental conditions (wind turbulence). The above physical description of the fire is captured in the model elaborated below.

3. Assumptions

The following assumptions are made in the formulation of the model:

(1) The time averaged mean geometry of the pulsating, turbulent diffusion fire can be represented by an enveloping cylinder of circular cross-section, tilted down wind, at winds above a critical wind speed (dependent on the diameter and burning rate).

(2) The axial fire plume length (or height) over which all vapors generated by the evaporating liquid pool are burnt is represented by a "mean visible plume length" and is calculated using the correlation by Thomas [23]. This correlation results in the plume length to diameter ratio varying as $D^{-1/3}$. In Appendix A it is shown that this is the correct representation (various fire height correlations in the literature and their incorrect application to large diffusion fires have been discussed by Raj [1]).

(3) The air entrainment rate is independent of the wind speed and depends only on the internal updraft velocity of gases inside the fire. Also, only a fraction of the mass of air entrained at any section is burned with its corresponding stoichiometric mass of fuel at that section. The value of this fraction is assumed to be constant throughout the burning plume of the fire.

(4) The fire emits uniformly in all directions at the same surface emissive power (SEP) at a given axial length from the base. The SEP, however, varies axially.

(5) Thermal radiation emission is uniform (i.e., the surface emissive power – SEP – is constant) near the base of the fire, over an axial length of fire equal to the clean burn-

ing zone length (L_C). This lower zone SEP represents the maximum value for the fire SEP.

(6) In zones 2 and 3 it is assumed that the inner core "hot flame" will be visible for a fraction of the time and for the other part of the time the flame core is shrouded by black smoke. However, since the smoke transmissivity is dependent upon the smoke concentration a part of the inner flame radiation will pass through the smoke layer. The fraction of the time the inner flame is visible is represented by a probability and this probability value decreases with increase in height (or axial distance from base).

(7) In the intermittency zones the overall surface emissive power is a linear, weighted sum of the maximum SEP and the smoke transmitted SEP. The weighting factor is the probability that at any time a given fraction of the cylindrical surface area is "open" so that the inner burning core of the fire can be "seen."

4. Details of the model

4.1. Fire plume length (L_F)

The following correlation due to Thomas [24] is used to calculate the average visible plume length for a fire of diameter D. [That the L/D ratio is proportional to the 2/3 power of the combustion Froude number (F_C), or proportional to $D^{-1/3}$ in windless condition is demonstrated in detail in Appendix A. Other correlations have been published in the literature based solely on experimental data curve fit and, in some cases, without adequate explanations of the physical basis of such correlations, Moorhouse [7] being an example.]

$$\frac{L_F}{D} = 55 F_C^{2/3} \quad \text{for } U^* \leq 1 \tag{1a}$$

$$\frac{L_F}{D} = 55 F_C^{2/3} (U^*)^{-0.21} \quad \text{for } U^* > 1 \tag{1b}$$

where,

$$F_C = \frac{\dot{m}''}{\rho_a \sqrt{gD}} = \text{combustion Froude number}$$

$$= \text{dimensionless burning rate} \tag{2}$$

and

$$U^* = \frac{U_{wind}}{[(\dot{m}''/\rho_a)gD]^{1/3}} = \text{dimensionless wind speed} \tag{3}$$

4.2. Axial length of the lower clean burning zone (L_C)

Heskestad [25] data indicates a correlation for the length of the intermittent zone (L_I) with the combustion Froude number F_C (for $7.5 \times 10^{-4} < F_C < 2.5 \times 10^{-1}$) as follows:

$$\frac{L_I}{L_F} = 0.167 - 0.25 \log_{10}(F_C) \tag{4}$$

We assume a form similar to the one in the above correlation for the intermittency zone but with a slight modification to conform to the data from 35 m diameter Montoir LNG fire test results

---

[3] It is noted that all liquid hydrocarbon fuels have about the same heating value per unit mass (within 10%). Also in all turbulent diffusion fires, the total mass of air entrained by the time the combustion is complete is about the same (about 10–15 times the stoichiometric mass value). If the radiative output to the outside is curtailed due to smoke shrouding, it stands to reason to expect that the fire temperature in all fuel fires to be about the same, within about 10%.

(Malvos and Raj [14]). It is seen in these tests that the bottom clean burning zone (L_C) near the base of fire is very small and can be represented by the following equation:

$$\psi = \frac{L_C}{L_F} = \left(1 - \frac{L_I}{L_F}\right) = 0.75 + \log_{10}(F_C^{1/4}) \tag{5}$$

The above formula will make the bottom clean burning zone length (L_C) to be zero for $F_C = 10^{-3}$ (which, for a LNG fire on water will be of the order of 3000 in diameter!).

4.3. Absorption of radiation by smoke

The presence of smoke in a fire results in the absorption of thermal radiation emission and a reduction in the effective emissive power. It is assumed that in the inner regions the fuel is burning at the same mean temperature, irrespective of the axial location within the visible plume. That is, the radiation emission internally within the fire is the same at all axial distances. However, the smoke that is produced by combustion chemistry under reduced oxygen concentrations ("anoxia" or lack of enough oxygen for complete combustion) transmits to the nominal flame surface only a fraction of the radiation produced inside the fire body. We define an effective emissive power for smoke (i.e., the emission from the cylinder surface shrouded by smoke layer) in the following equation:

$$E_S = E_b \tau_s \tag{6}$$

where,

$$\tau_s = \text{transmissivity of smoke} = e^{-(k_m C_s L_b)} \tag{7}$$

where E_S is the effective surface emissive power in the smoke (kW/m^2), E_b the surface emissive power at the lower regions (kW/m^2), k_m the specific soot extinction area (m^2/kg), C_s the mass concentration of smoke in the flame gases (kg smoke/m^3) and L_b is the beam length $= 0.63D$, for cylindrical fires (m).

It can be shown that the soot concentration C_s (kg/m^3) is related to the burning efficiency of the fuel (β), the heat of combustion of the fuel (ΔH_c), the stoichiometric air to fuel mass ratio (r) and the soot mass yield per unit mass of fuel burned (Y) by the formula:

$$C_s = \rho_a Y \frac{1}{1 + (r/\beta) + (\Delta H_c/C_a T_a)} \tag{8}$$

where β is the combustion efficiency factor (fraction of the mass of air entrained at any location that burns with its stoichiometric equivalent mass of fuel)—assumed as a constant throughout the combustion zone.

Notarianni et al. [17] measured the smoke production in crude oil fires of diameters from 0.085 m to 17.2 m and found that smoke yield, Y (mass% of burnt fuel that is emitted as smoke) increases as the diameter of the fire increases. The data for the mass fraction smoke yield (Y in %) versus fire diameter (D in m) presented by these researchers can be correlated (for crude oil fires) by the following equation:

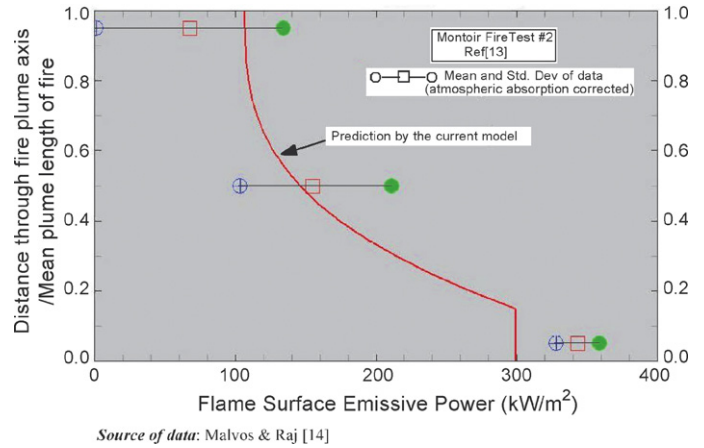$$Y = 9.412 + 2.758 \times \log_{10}(D) \quad (D \text{ in m}) \tag{9}$$

Fig. 3. Comparison of the model result and the data from narrow angle radiometer measurement of the emissive power variation with height above firebase.

There are no experimental data for the soot yield in large methane (or LNG) fires. However, as will be shown later based on the test results of 35 m diameter Montoir LNG fire tests and the model proposed for the variation of the emissive power with distance (axial location) through the fire plume it is seen that the above correlation may be appropriate for large methane fires also. This assumption may, or may not, be valid; only experimental results can provide answers.

4.4. Emissive power variation through the fire axial length

In the intermittency zone, the surface emissive power varies because of smoke shrouding. We assume that the rate of intermittency varies between 0% (i.e., there is no smoke obscuration) at the top of the "clean burning zone" to 100% (i.e., full smoke obscuration) at the top of the intermittency zone. In other words the probability of realizing the maximum SEP varies from 1 at the bottom of the intermittency zone to 0 at the top of the intermittency zone. This probability can also be interpreted as the fraction of the time that the outer layers of the cylindrical fire show the "inner core" thus radiating at the maximum SEP; the remainder of the time the emission is from the smoke layers. The above concept is mathematically expressed as follows.

The probability of being exposed to the maximum SEP value (E_{max}) at any axial position is set to p. In the intermittency region "p" is assumed to be given by the following polynomial variation, of order "n", with the axial length (from the flame tip). The value of "n" is determined from the "best fit" to the data from the 35 m diameter, Montoir LNG fire tests (see Fig. 3):

$$p(\xi) = \left[\frac{1 - \xi}{1 - \psi}\right]^n \quad \text{for } \psi \le \xi \le 1 \tag{10a}$$

$$p(\xi) = 1 \quad \text{for } 0 \le \xi \le \psi \tag{10b}$$

$$\xi = \frac{Z}{L_F} = \frac{\text{length along the fire axis}}{\text{visible fire plume length}} \ge \psi \tag{11}$$

$$\psi = \frac{L_C}{L_F} = \text{ratio of "clean burn zone"}$$

axial length and the visible plume length　　　　(12a)

Using Eqs. (4) and (5) it can be shown that

$$\psi = \frac{L_c}{L_F} = 0.75 + 0.25 \log_{10}(F_C) \tag{12b}$$

The value of ψ, for fires of several meters in diameter is generally between 0.15 and 0.25.

The axial variation of the surface emissive power (SEP) over the entire visible plume length of the fire can then be represented as follows:

$$E(Z) = E_b \quad \text{for } 0 \le \frac{Z}{L_F} \le \psi \tag{13a}$$

$$E(Z) = pE_b + (1-p)E_S(Z) \quad \text{for } \psi \le \frac{Z}{L_F} \le 1 \tag{13b}$$

where E_b is the emissive power of the brightest part of the fire (near the base), $E_S(Z)$ the emissive power of the smoke layer (from Eq. (6)) and $p(Z)$ is the probability that at any give time the inner fire is visible at height Z (see Eqs. (10a) and (10b)).

The overall mean SEP is then obtained by integrating E in Eqs. (13a) and (13b) from $Z=0$ to $Z=L_F$. That is,

$$E = \int_{\xi=0}^{\xi=1} E(\xi)\,d\xi \tag{14}$$

Substituting Eqs. (13a) and (13b) in (14) and using the definition of p from Eqs. (10a) and (10b) it can be shown that:

$$\frac{\bar{E}}{E_b} = \psi + \left\{ \frac{1 + n\tau_s}{1 + n} \right\}(1 - \psi) \tag{15}$$

It is seen from the data shown in Fig. 3 that the best value for n is 3.

The fire base emissive power will depend on the size of the fire. The China Lake experiments (Raj [11]) indicated that the 13 m diameter LNG fire on water was not radiating like a blackbody at the hot gas temperature. Based on the analysis of the spectral data from these tests the fire base emissivity was calculated to be 0.61 (Raj et al. [8], Raj [11]). The mean emissivity (wavelength independent) can be related to the fire base diameter as follows:

$$\varepsilon = 1 - e^{-D/D_{opt}} \tag{16}$$

where ε is the overall fire emissivity, D the fire base diameter (m) and D_{opt} is the optical depth (or path length) (m).

Based on Eq. (16) and the 13 m diameter LNG fire data discussed above, the optical depth of LNG pool fire is calculated to be 13.81 m. Therefore, any fire of diameter less than, say, 2.5 times the optical depth radiates at its bottom at less than 92% of the maximum emissive power consistent with the gas temperature (found to be about 1500 K in the China Lake fire). We, therefore, use for calculating the base emissive power (E_b) the following equation:

$$E_b = E_{max}(1 - e^{-D/D_{opt}}) \tag{17}$$

The value of E_{max} is set to $325\,\text{kW/m}^2$, consistent with the measured narrow angle radiometer data from the Montoir tests (Malvos and Raj [14]).

5. Results

Calculations are performed to evaluate the mean surface emissive power of different diameter LNG pool fires. These results are presented in Table 1. The values assumed for some of the parameters are also indicated in the table. Also shown in the table are the experimental values for the mean emissive power as calculated from the wide-angle radiometer measured heat flux values in field tests corrected for atmospheric absorption and the visible fire height calculated using Thomas' correlation (Eqs. (1a) and (1b)).

The variation of the emissive power with axial distance through the length of the visible plume of a 35 m diameter fire for the conditions of test 2 in the Montoir series is shown in Fig. 3. The narrow angle data (indicated in Fig. 2) are also plotted in Fig. 3. Also plotted for comparison in Fig. 3 are the model predicted results for a 35 m LNG fire on land.

6. Discussions

This paper has attempted to describe a semi-empirical model for predicting the thermal radiation output from large turbulent diffusion fires on flammable liquid pools. Observations from large tests with LNG (at 35 m diameter), field tests with other higher hydrocarbon fuels (JP-5 at 15 m diameter) and large oil spill fires on the ocean have indicated clearly that large fires, irrespective of the fuel involved, burn with the production of copious amount of smoke. The "density" of smoke generated seems to be a function of the fuel characteristics and the fire size. It is theorized that the latter effect is in reducing the oxygen concentration in the inner (radial) regions of the fire. Unfortunately, there are no experimental data on the values of concentrations of oxygen, fuel vapor, combustion product gases, smoke density and their variation axially and radially. The lack of data is especially true for large LNG fires.

The motion picture records from the largest LNG fire tests that have been conducted to date (in Monotoir, France, 1987), clearly indicate that a large LNG fire burns with production of very large amount of soot. Also observed is that the dynamics and visual characteristics of such a (LNG) fire are not much different from that of an oil fuel fire (see photographs comparing 35 m LNG fire and a pool fire of refined crude oil released from the rupture of a pipeline, Raj [1]). One of the important observations from large fire behavior is that the burning is pulsed with rising thermals of burning gas (in the form of large eddies). In addition the smoke, at heights greater than a critical level, envelops the entire inner burning region, thereby curtailing the radiant heat output from those sections of the fire to the outside. Also noticeable both in the film of 35 m LNG fire tests and in narrow-angle radiometer readings taken at three different heights is that the fraction of the time the "inner burning fire" is visible through the shrouding smoke layer decreases with increasing height. Unfortunately, there are no published data in the literature on the magnitude of

Table 1
Comparison of model predicted[a] SEP with experimental data

Fire diameter (m)	Surface on which LNG boils	Froude number (F_c) (×10⁻³)	Soot mass yield (Y)[b] (%)	Soot concentration (C_s) (kg/m³) (×10⁻⁴)	Fractional length of the "clean burning zone" (ψ)	Soot[c] transmissivity (τ_s) (×10⁻²)	Mean SEP over the visible fire plume height (E_{avg})		Remarks
							Current model result (kW/m²)	From field tests (kW/m²)	
15	Water	9.606	12.7	3.328	0.196	66.4	172	185–224	Raj, et al [8], China Lake tests
20	Land	8.319	13.0	3.419	0.180	57.12	183	140–180	Mizner and Eyre [16]
35	Land	6.288	13.7	3.595	0.150	35.7	177	175 ± 30	Malvos and Raj [14], Montoir tests
100	Land	3.720	14.9	3.926	0.093	4.0	113	–	Potential size of future pool fire tests
300	Water	2.148	16.2	4.272	0.033	0.0028	90	–	Estimated pool size due to 1/2 tank content spill (12,500 m³ LNG) from an LNG ship

[a] Assumed parameter values: $r = 17.17$ for CH$_4$; $\beta = 0.06$; $k_m = 130$ m²/kg; $E_{max} = 325$ kW/m²; $T_a = 293$ K.
[b] Notarianni et al. [17] correlation for smoke yield.
[c] Assumed optical depth at bottom of LNG fire = 13.8 m.

this intermittent visibility of the inner burning region through the smoke layer and the variation of the fraction of the time the inner fire is visible as a function of the fire height and other characteristics of the fire including its size (diameter), properties of the fuel, etc. These experimental observations, albeit from a limited number of tests, are included in the model, with several simplifications.

The rate of smoke production, expressed as a constant mass fraction (Y) of the fuel burned, used in the model is based on a dimensional data correlation from one set of tests with crude oil fires of varying diameter up to a maximum of 17.2 m (Notarianni et al. [17]). No such data (i.e., fraction of the mass of fuel converted into unburnt smoke or carbon particles) are available for methane, propane or any other fuel fires. Not available also are the black smoke extinction coefficients for the smoke generated from a methane fire. It is, however, assumed that the IR spectral average extinction coefficient value depends on the characteristics of the fire. In view of the above gaps in knowledge, the model uses the best available value for each of the physical parameters such as the smoke yield mass fraction (Y, as a function of the diameter), the extinction coefficient for absorption of thermal radiation by smoke particles (k_m), and the excess air entrained in large fires (β). It is noteworthy that the correlation for the smoke yield does not explicitly indicate its dependence on the burning rate. The diameter dependence can be considered as a proxy to the air mixing inefficiencies and the starvation of the central parts of the fire of oxygen for combustion. However, it can be argued that for a given diameter if the rate of vapor flow into the fire is increased a higher percent of the fuel should be converted to smoke. This is due to the reduced oxygen concentration and correspondingly increased concentration of fuel. Thus a higher vapor evolution rate will lead to further inefficient combustion and, hence, the production of a greater fraction of the fuel mass into unburnt carbon (smoke). This argument, if true, will lead to a more smoky LNG fire on water compared to a fire on land of the same diameter. Such a fire behavior leads to the conclusion that hazard distance from LNG fires on water will be less than that from a land fire of the same diameter.

The parameter β represents the combustion efficiency at any layer of burning; that is, efficiency (or probability) with which the air entrained at the particular layer burns with its stoichiometric equivalent mass of fuel vapor. (The expression $1/\beta - 1$ represents the mass of excess air required for the complete combustion of the fuel vapor emanating from the pool—for more details of this, see Raj [26].)

The model proposed includes an assumed variation of the fraction of the time the inner core is visible through the smoke shield and the variation of this fraction with the distance along the fire plume axis. This fraction (also referred to as "p" the probability of "seeing" the inner burning regions) is assumed to increase with the distance backwards from the visible tip of the fire as some power of the distance (see Eq. (10a)). A similarity profile for the variation of p with non-dimensional distance is assumed. Unfortunately, there are no experimental data from either large fires in the field or smaller, laboratory size fires (which have much less of the smoke shielding effect in LNG fires) on which to base the exact variation of "p" with the axial

length in the smoky parts of the fire. Various similarity profile index (i.e., the exponent on the non-dimensional distance along the fire axis) values were tried. The finally chosen distribution of "*p*" was with a cubic variation shown in Eq. (10a). This value of the exponent (a value of 3) was the one that fit the model predictions with lowest error both with the measured variation of the NAR data along the axis (Fig. 3) and the average emissive power measured with the wide angle radiometers (see Table 1) from the 35 m diameter Montoir LNG fire tests (Malvos and Raj [14]). Whether this is the correct representation of the variation of the "visibility" of the inner burning regions in all large fires cannot be determined until additional experimental measurements are made or an effort is undertaken to review films of past large scale field size fire experiments (with other fuels) and obtain the necessary information. Such an effort has not been done, and was not done as a part of this modeling effort.

The data presented in Fig. 1 are the 'as measured' narrow-angle radiometer (NAR) readings taken at the bottom, mid height and the top of a 35 m diameter LNG pool fire on insulated concreted dike in test 2 of the Montoir series. The *x*-axis represents the uncorrected (for atmospheric absorption) emissive power of the fire measured by the NAR. The *y*-axis indicates the fraction of the time during the measurement in which the particular value of the emissive power was recorded. The data presented represent, for each location on the fire, a recording duration of 5.8 s during which a total of 145 measurements were made. Two important features are noticeable from the data presented. First, the mean value of the emissive power varies drastically from the bottom of the fire to the top (by a factor of about 5). Second, the statistical distribution of the measurements shows very narrow dispersion (low ratio of standard deviation to mean) at the bottom of the fire and high dispersion at the top of the fire. This can be interpreted as the fact that at the bottom of the fire, most of the heat is being emitted continuously, un-obscured by smoke layers. That is, the bottom layers burn "clean". However, as one goes up in height, the dispersion is higher with considerable scatter in the measured emissive power, although the mean value is reduced significantly. That is, the higher one goes up the larger is the shrouding effect by the smoke of the inner burning regions but the greater is the variation in the smoke layer aperture that "opens" and "closes". One can attribute this to a higher level of the intensity of turbulence in higher layers.

The experimental NAR data shown in Fig. 3 are the data in Fig. 1, which have been corrected for the IR radiation absorption by the atmosphere at the conditions prevailing during the test (54% relative humidity and 21 °C, with the NAR being located 155 m from the edge of the dike). Only the corrected mean and standard deviation values as a function of the height are plotted. The atmospheric transmissivity factors for the test conditions are calculated to be 0.67 to the bottom of the fire, 0.668 at mid height and 0.661 at the top (for a detailed discussion of the various atmospheric transmissivity models and their accuracies, see Lees [27]). Also plotted in Fig. 3 is the variation of the emissive power with height predicted by the model.

The model results are based on the assumption that the black body emissive power of the "clean burning" region (at the base of the fire) is 325 kW/m². The actual emissive power at the base of the fire is lower because the 35 m diameter fire is not optically thick. The base emissive power is calculated to be 299 kW/m². This value is in keeping with the mean value from other NAR data focusing on the bottom of the fire. The model further assumes that the height of the lower clean burning zone is given by Eq. (5) in which the properties of methane and 35 m diameter values are used. The correlation results in a height of the bottom "clean and bright" burning region to be 11.3 m. No data have been published on the actual variation of the NAR readings close to the bottom of the fire; however, based on known information (Malvos and Raj [14]) it appears the bottom "bright region" is about 10 m in test 2. The correlation indicated in Eq. (5) was some what modified from that in the literature to coincide with the Montoir LNG test 2. It should be noted however, that the correlation in Eq. (5) predicts reasonably well the lower bright region of a 15 m diameter LNG fire (on water) tested in China Lake (Raj et al. [8])—this region is predicted as 25% of visible plume height (of 50 m).

The values of other parameters used in the model (β, k_m, r) are indicated in Table 1. The results of the model agree reasonably well with the experimental NAR data. It should be noted that the NAR data provides information on only a specific spot (of about 1.5 m diameter) on the nominal surface of the fire, whereas, the model predicted value should be considered as a mean value at a given height. Also, there is uncertainty as to the exact height at which the NARs were looking and because of slight wind the line of sight to the spot "seen" by the NAR may not have intersected the fire axis; thus the NAR readings may, in fact, represent a slightly off center value of the emissive power (with the effect of the cosine of the angle of the spot area with respect to the line of sight being important). There are uncertainties in specifying which exact part of the fire the NARs were pointing to. The model predicts slightly lower values for the emissive power at the base compared to measured values. Again it is emphasized that the model provides a "mean" value for the emissive power over a horizontal section at any height where as the NARs 'look' at a single spot. The model predicts higher values with height than is indicated by the data, in spite of the fact that the crude oil values for smoke yield and propane values for the smoke extinction coefficient were used (one expects that using crude oil smoke yield correlation one would get a lower emissive power at the top parts of the fire). It is not certain why this slight discrepancy between the model and the LNG fire NAR data occurs. It may be due to the recipe assumed for the distribution of the probability of "inner core view" assumed in Eqs. (10a) and (10b); may be a faster rate of decrease of this probability with height is appropriate. However, any such assumption at this time will only be a theoretical exercise without much comparable data. There is, therefore an important need to obtain such intermittency data from large, outdoor fires.

The average value over the visible plume length of the calculated emissive power distribution along the fire axis has been obtained for four different size fires, both on land and on water. These include hypothetical LNG fires of a 100 m diameter on land and a 300 m diameter fire on water. The calculated results together with the experimental mean values for two fire sizes actually tested are indicated in Table 1. It is seen that the model

predicted mean emissive power for the 15 m fire is slightly lower than measured values, whereas, for the 35 m diameter fire it is within the range of measured values. Considering the uncertainties in the values of parameters used in the model and their applicability to a methane (or LNG) fire, the small differences in the predicted and measured values are within the acceptable range. Table 1 results illustrate that as the fire diameter increases the mean emissive power over the entire visible fire plume length becomes smaller. As can be seen, the mean emissive power for a 300 m fire is only about 60% of that of a 15 m diameter fire!

It is also noted that in the current model formulation the probability (p) of radiation emission from the inner hot core varies as the cube of the distance from the tip of the flame—see Eq. (10a). Therefore, as the diameter increases significantly, the average value of the emissive power over the "visible" flame asymptotically reaches a value of $E_b/4$. However, this result is just academic. As the diameter increases, according to Eq. (1a) or (1b), the visible length to diameter ratio becomes smaller and smaller (and becomes zero in the asymptotic limit). The flame length does not, however, become zero. The soot emissive power (E_S from Eqs. (6) and (7)) becomes asymptotically zero. Hence we have, asymptotically a fire with zero visible flame length/diameter but with finite "average" emissive power (the averaging this case is over zero length). Since the view factor is dependent on the L/D ratio, the ratio of the hazard distance/diameter decreases continuously with increase in diameter and will reach a limit value consistent with the specified hazard heat flux.

The result of this model clearly indicates that as the fire size increases the mean emissive power decreases. Also, as the fire diameter increases, the fire plume length to diameter ratio decreases. Therefore, the hazard distance, as a fraction of the fire diameter, for any specified hazard heat flux decreases as the diameter increases. The LNGFIRE3 model specified in US Government regulations and those specified in NFPA 59A standard (LNGFIRE3 and the point source models) for LNG do not consider the issue of reduction in the total energy out put (as a fraction of the combustion energy released) due to smoke effects. The result of using the current regulatory model for LNG or other large fire hazard evaluation is the prediction of large distances (1–2 km) for people hazards. Secondly, as seen from the above model and the results of large scale tests with LNG the bottom part of the fire radiates at a much higher level than the parts at the top. This phenomenon is extremely important to note in the calculation of hazard distances from dike fires in LNG or other fuel storage facilities (surrounded by a high enough dike wall). The presence of a dike wall of even relatively small height (say, 10 m) cuts out a very significant level of radiation from the fire to the surrounding. The hazard distance calculated using the emission from the parts of the fire visible above the dike wall is likely to be a factor of 1.5–2 less than that obtained from currently used models.

7. Conclusions

The following conclusions are drawn from the model reported in this paper:

(1) A semi-empirical model to predict the thermal radiation output from large hydrocarbon liquid fuel pool fires has been proposed which takes into consideration the formation of smoke, its effect (by shrouding the inner burning region) in reducing the thermal output into the surroundings.

(2) The model assumes a constant emissive power zone at the bottom of the fire. The height of this zone varies with the properties of the fuel, the size of the fire and the evaporation rate. The variation of the emissive power with height above this zone has been modeled by assuming a probability distribution for the fraction of the time the inner core of burning fire is visible through the smoke shroud.

(3) The results of the model have been compared with the only available (narrow angle radiometer) data for the measured variation of the emissive power with height. The model results track this variation reasonably well, given the uncertainties in the model assumptions and in the data.

(4) The model also predicts the measured mean emissive power from 15 m and 35 m LNG fire tests within the accuracy that can be ascribed to the model.

(5) The model is realistic in its treatment of the actual dynamics and phenomena observed in all large hydrocarbon fuel fires, including the very important one relating to smoke production and obscuration of the burning regions of the fire. In this regard it may be better than models used for LNG fire hazard determination (such as LNGFIRE3), which are based on the use of a single mean emissive power value, independent of fire size.

(6) The use of the model proposed has significant implications for the calculation of more reasonable hazard distances as opposed to the large hazard distance predictions of the currently used (or required to be used) fire models.

Appendix A. Relationship between visible fire plume height, diameter and burning rate

Observations from fire experiments as well as accidental fires over burning pools of hydrocarbon liquid fuels indicate that the visible fire plume is very columnar, for fires up to about 50 m diameter. That is, the visible fire looks very much like a vertical (in low wind conditions), burning and radiating plume. The visible plume height is not fixed in time but pulsates up and down about a mean height. The pulsation rates change with the diameter. Also, as the fire diameter becomes bigger, the entire dynamics of burning in the upper layers change due to the formation of a toroidal vortex. The puff type burning (with the toroidal vortex) results in recirculation of the burnt gases, dilution of air and formation of smoke, which is brought out to the surface by the toroidal circulation. The net effect of this is to make the combustion less efficient at the upper layers of larger fires. While the height up to which the combustible gases burn inside the fire may not be affected (other than by the air entrainment dynamics), the thermal radiation output from the upper layers is considerably reduced.

The observation that liquid pool fires burn in a long column of relatively same diameter from the base to the tip of the observable flame sheet is used in formulating the physical problem

described below. Also used in the analysis below is the concept that only a mass fraction (β) of the air entrained up to a given height "burns" with its stoichiometric equivalent fuel. This "inefficiency in combustion" continues until there is no more fuel vapor left in the fire to burn. The height at which all of the fuel is exhausted is considered to be the top of the visible flame height. This concept has been successfully used (Raj [26]) in a mathematical model to explain the experimentally measured centerline temperature and gas velocity variation with height in a 15.2 m diameter JP-4 pool fire.

A.1. Analysis

A fire shown schematically in Fig. A1 is considered. The vertical extent of the visible plume of the fire is represented by a mean flame height L_F. Air for combustion is entrained from the atmosphere along the sides of the visible plume boundary. A fraction of the mass of air entrained "burns" in stoichiometric proportion with fuel vapor flowing at that height. The remainder of the fuel vapor traveling up in the fire plume burns with the same fraction of the air entrained in the next layer. The top of the visible plume is represented by the height at which all of the fuel mass emanating at the "pool surface" is stoichometrically burned with air. That is, the gases that are in the updraft at the level of the top of the visible fire plume consist of products of combustion and excess air only.

In addition to the physical description above (and the assumptions that are part of the description) the following additional phenomena are assumed:

(1) The entrainment of air occurs at the periphery of the column fire.
(2) The air entrainment rate at any horizontal section (at height Z) is proportional to the local vertical upward velocity of gases at that height. The local upward velocity used for entrainment is the velocity of gases averaged over the horizontal section of fire at height z.
(3) The mean upward velocity of gases at any height Z is proportional to the square root of Z. (This is borne out by data
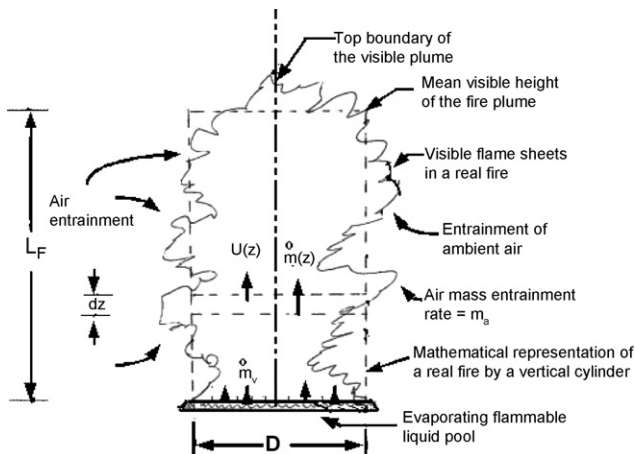

Fig. A1. Schematic representation of a columnar fire over a burning hydrocarbon liquid pool.

from large field tests with other hydrocarbon fires where such velocity measurements have been made.)

Referring to Fig. A1, we write the mass flow rate of gases within the visible plume, at any height Z above the base of the fire[4]

$$\dot{m}(Z) = \dot{m}_f + \dot{m}_a(Z) \tag{A1}$$

where $\dot{m}(Z)$ is the mass flow rate at section at height Z, $\dot{m}_f$ the mass flow rate of fuel at fire base and $\dot{m}_a(Z)$ is the mass rate of air entrainment up to height Z.

From the assumption on the entrainment rate,

$$\dot{m}_a(Z) = \rho_a \alpha \bar{U}(Z) \pi D Z \tag{A2}$$

where α is the air entrainment coefficient (of the order of 0.1) and $\bar{U}(Z)$ is the mean velocity of gases over the height 0 to Z.

The last term on the RHS of Eq. (A2) represents the side area of the fire over which air is entrained.

It is known from the literature and analyses (Raj [26]) that the mean upward velocity of gases at any height is given by the expression:

$$\bar{U}(Z) = \frac{2}{3} \sqrt{2g \frac{\Delta\rho}{\rho_a} Z} \tag{A3}$$

with

$$\frac{\Delta\rho}{\rho_a} = \frac{\rho_a - \rho}{\rho_a} \tag{A4}$$

The term $\Delta\rho/\rho_a$ represents the fractional decrease in the density of gases due to combustion. It is later shown that this term is a constant and does not vary (to the accuracy of our assumptions) in the Z-direction within the fire. The constancy of this term is a result of the assumption that a mass fraction β of the mass of air entrained up to a height Z "burns" with its equivalent stoichometric mass of fuel vapor.

The top of the visible flame represents the section by which all of the fuel generated at the base of the fire is consumed by burning. That is at $Z = L_F$ we have:

$$r\dot{m}_f = \beta \dot{m}_a(L_F) \tag{A5}$$

where r is the Stoichiometric air to fuel mass ratio (17.17 for CH_4) and β is the mass fraction of air entrained that burns with fuel, stoichiometrically.

Substituting Eqs. (A2) and (A3) in Eq. (A5) and setting $Z = L_F$, and rearranging, we get:

$$\beta \alpha \rho_a \left(\frac{2}{3}\right) \sqrt{2g \frac{\Delta\rho}{\rho_a}} L(\pi D L_F) = r\dot{m}_f'' \frac{\pi}{4} D^2 \tag{A6}$$

with $\dot{m}_f''$ representing the mass evaporation rate from the pool per unit area. Eq. (6) can be written in a modified way as follows:

$$\frac{L_F}{D} = \left[\frac{3r}{8\sqrt{2}\beta\alpha\sqrt{\Delta\rho/\rho_a}}\right]^{2/3} \left(\frac{\dot{m}_f''}{\rho_a\sqrt{gD}}\right)^{2/3} \tag{A7}$$

---

[4] See nomenclature for the definition of symbols.

A.2. Evaluation of the fractional density deviation term $(\Delta\rho/\rho_a)$

Assuming that the gases are perfect with the same molecular weight

$$\frac{\Delta\rho}{\rho_a} = \frac{\Delta T/T_a}{1 + (\Delta T/T_a)} \tag{A8}$$

where $\Delta T = (T - T_a)$ temperature rise of the gases due to the heat generated by combustion.

Hence, in the L/D correlation in Eq. (6) the fractional increase in the temperature of the burnt gases and excess air mixture relative to the outside air temperature can be substituted (from Eq. (A8)) for the fractional density decrease $(\Delta\rho/\rho_a)$.

Consider a horizontal plane at height Z above the base of the fire. Using the definition of the parameters indicated earlier we show that:

$$\dot{m}_f(Z) = \beta\frac{\dot{m}_a}{r} \tag{A9}$$

where $\dot{m}_f(Z)$ is the mass rate of fuel burning up to height Z.

The total heat production rate by combustion up to height Z is therefore:

$$\dot{Q}(Z) = \dot{m}_f(Z)\Delta H_c = \beta\frac{\dot{m}_a}{r}\Delta H_c \tag{A10}$$

Assuming that all gases have the same mass specific heat, we write the enthalpy equation for the gases at a height Z plane,

$$\{\dot{m}_{f,0} + \dot{m}_a(Z)\}C_aT(Z) = \{\dot{m}_{f,0}C_fT_f(0) + \dot{m}_a(Z)C_aT_a\} + \dot{Q} \tag{A11}$$

where $\dot{m}_{f,0}$ is the mass flow rate of fuel at the base of the fire.

Assuming (without significant loss of generality) that $C_fT_f(0) = C_aT_a$. Substituting Eq. (A8) and Eq. (A10) in Eq. (A11) and rearranging, we show that:

$$\frac{\beta}{r}\frac{\Delta H_c}{C_pT_a}\frac{\dot{m}_a}{(\dot{m}_{f,0} + \dot{m}_a)} = \frac{T(Z) - T_a}{T_a} = \frac{\Delta T}{T_a} \tag{A12}$$

It is known that the mass of air entrained up to any height Z (for $Z > 0.1D$) is substantially larger than the mass flow rate of vapors at the fire base (for example, the total mass of air flowing through the top of the visible flame is estimated to be an order of magnitude higher than the stoichiometric value of $r = 17.17$; that is, the air entrainment is about 170 times the mass flow rate of vapors at the surface of the pool). Hence, the ratio $\dot{m}_a/(\dot{m}_{f,0} + \dot{m}_a)$ can be considered to be unity. In this case, Eq. (A12) indicates that the ratio of temperature rise of the gases and air temperature is constant for all heights.

Eq. (A6) is written in a non-dimensional form as follows[5]:

$$\frac{L_F}{D} = AF_c^{2/3} \tag{A13}$$

where,

$$F_c = \text{combustion Froude number} = \left(\frac{\dot{m}_f''}{\rho_a\sqrt{gD}}\right) \tag{A14a}$$

$$A = \text{constant factor} = \left[\frac{3r}{8\sqrt{2}\beta\alpha\sqrt{\Delta\rho/\rho_a}}\right]^{2/3} \tag{A14b}$$

We now define,

$$D = \text{Damkohler number} = \frac{\Delta H_c}{C_aT_a} \tag{A15}$$

Substituting results of Eqs. (8), (12a), (12b) and (15) in Eq. (14) we get:

$$A = \left[\frac{9}{128\alpha^2 D}\right]^{1/3}\frac{r}{\beta}\left(1 + D\frac{\beta}{r}\right)^{1/3} \tag{A16}$$

Eq. (A13) shows that L_F/D ratio of the fire varies as the 2/3 power of the non-dimensional burning rate or the combustion Froude number. This exactly the result indicated by Thomas [24]. Heskestad [25] also has published the correlations for the L_F/D ratio for a wide range of Froude number; his correlation, though has a different mathematical formula, follows the 2/3 law in the applicable values (for large fires) of the combustion Froude number. The correlation of Thomas indicates the following:

$$A = 55 \tag{A17}$$

The above value is based on wood crib fire experimental data. This value of A is used below to estimate the value of the combustion efficiency factor β.

A.3. Value of the combustion efficiency factor β

The following values for the thermal and combustion properties of methane and other parameters are used

r	Air to fuel mass ratio for stoichiometric combustion	17.1674
ΔH_c	Heat of combustion	50.02 MJ/kg
C_a	Specific heat of air	1000 J/kg/K
T_a	Air temperature	293 K
α	Air entrainment coefficient	0.1
D	Damkohler number $= \Delta H_c/(C_aT_a)$	170.05

Substituting the above values on the RHS of Eq. (A16) and setting $A = 55$ results in a value of $\beta = 0.1454$. That is, by the time the combustion of all of the fuel is complete about $1/\beta = 6.88$ times the stoichiometric mass of air is ingested into the fire. This is in keeping with the experimental observations reported by Thomas that an order of magnitude more air than the stoichiometric mass is entrained into the fire. The same approach when used with the JP-4 fire data results in $\beta = 0.06$. Hence, there is

---

[5] If the fire plume is assumed to be an inverted frustum of a cone with base

diameter equal to the fire diameter and the cone angle is α then it can be shown that the Eq. (A13) changes to

$$\frac{L_F}{D}\left\{1 + \frac{\alpha}{2}\left(\frac{L_F}{D}\right)\right\}^{(2/3)} = AF_c^{2/3}$$

For most fires of interest with L_F/D in the 0.5–3 range, and $\alpha = 0.1$, the second term in the { } brackets is small compared to 1 and can be neglected.

some uncertainty as to where the "visible fire plume" ends on a statistical mean basis.

Also, it can be shown from the above value of β and the relationships in Eqs. (A8) and (A12) that:

$$\frac{\Delta T}{T_a} = \frac{\beta}{r} N_E = 1.44 \quad \text{and} \quad \frac{\Delta \rho}{\rho_a} = 0.59 \qquad (A18)$$

A.4. Conclusions

(1) The analysis above shows clearly that for most liquid pool fires of hydrocarbon fuels that may occur due to accidents the height of the visible plume can be estimated by an equation (Thomas' modified equation). The *L/D* ratio of the fire varies as the 2/3 power of the combustion Froude number.
(2) The model developed provides a means of estimating the value of the constant factor for different fuels with known properties of the fuel and assumed efficiency of combustion.
(3) The model presented does not provide any means of indicating how the radiation output from the fire varies with height nor does it predict the chemistry that occurs within the fire (due to combustion inefficiencies).

References

[1] P.K. Raj, Large LNG fire thermal radiation-modeling issues and hazard criteria revisited, Process Safety Progr. 24 (3) (2005).
[2] H.G. May, W. McQueen, Radiation from large liquefied natural fires, Comb. Sci Tech. 7 (1973) 51–66.
[3] AGA, LNG Safety Program—Interim Report on Phase II Work, IS-3-1, American Gas Association, Arlington, VA, July, 1974.
[4] P.K. Raj, A.S. Kalelkar, Fire-Hazard Presented by a Spreading, Burning Pool of Liquefied Natural Gas on Water, Paper Number 73–25, Western States Section, The Combustion Institute, Fall Meeting, 1973.
[5] P.K. Raj, S. Atallah, D-2 thermal radiation from LNG spill fires, Adv. Cryogen. Eng. 20 (1974) 143.
[6] P.K. Raj, Calculations of Thermal Radiation Hazards from LNG Fires—A Review of the State-of-the-Art, AGA Transmission Conference, ST. Louis, Missouri, Paper Number 2, Session 18, May 18, 1977.
[7] J. Moorhouse, Scaling criteria for pool fires derived from large-scale experiments, the assessment of major hazards, I. Chem. E. Symp Series No. 71 (1982) 165–179.
[8] P.K. Raj, A.L. Moussa, K. Aravamudan, Experiments Involving Pool and Vapor Fires from Spills of LNG on Water, NTIS No. AD-A077073, USCG Report, Washington, DC 20590, 1979.
[9] M. Considine, Thermal Radiation Hazard Ranges from Large Hydrocarbon Pool Fires, Report No. SRD R297, Safety & Reliability Directorate, UK Atomic Energy Authority, Wigshaw Lane, Culcheth, Warrington, WA3 4NE, UK, October, 1984.
[10] C.L. Beyler, Fire hazard calculations for large, open hydrocarbon fires, in: The SFPE Handbook of Fire Protection Engineering, 3rd ed., National Fire Protection Association, Quincy, MA, 2002, Section 3, Chapter 11, pp. 3–268.
[11] P.K. Raj, LNG Fire Spectral Data and Calculation of Emissive Power, Presented at the International Symposium on Process Safety, Mary Kay O'Connor Process Safety Center, Texas A&M University, College Station, TX, October 25–26, 2005, J. Hazard. Mater., in press.
[12] R.K. Smith, Radiation effects on large fire plumes, in: Proceedings of the 11th International Symposium on Combustion, The combustion Institute, Academic Press, New York, 1967, p. 507.
[13] K.B. McGrattan, H.R. Baum, A. Hamins, Thermal Radiation from Large Pool Fires, NISTIR 6546, National Institute of Standards & Technology, U.S. Department of Commerce, Washington, DC, 2000.
[14] H. Malvos, P.K. Raj, Details of 35 m Diameter LNG Fire Tests Conducted in Montoir, France in 1987, and Analysis of Fire Spectral and Other Data, Paper Presented in Session T6005 LNG VI, Risk & Safety, AIChE Winter Conference, Orlando, FL, April, 2006.
[15] D. Nedelka, J. Moorehouse, R.F. Tucker, The montoir 35 m diameter LNG pool fire experiments, TRCP.3148R, in: Proceedings of the Ninth International Conference & Expo on LNG, LNG IX IX, Nice, France, 1989.
[16] G.A. Mizner, J.A. Eyre, Large scale LNG and LPG pool fires, in: Proceedings of the Institution of Chemical Engineering Symposium, Series No. 71, Manchester, April, 1982.
[17] K.A. Notarianni, D.D. Evans, W.D. Walton, D. Madrzykowski, J.R. Lawson, in: C.A. Franks (Ed.), Proceedings of the Sixth International Fire Conference on Smoke Production from Large Oil Pool Fires, Interflam 1993, Fire Safety, Interscience Communications Ltd., Oxford/London, England, March 1993, 1993, pp. 111–119.
[18] K.S. Narasimhan, P.J. Foster, The rate of growth of soot in turbulent flow with combustion products and methane, in: Proceedings of the Tenth International Symposium on Combustion, The Combustion Institute, 1965, pp. 253–257.
[19] H.S. Hura, I. Glassman, Soot formation in diffusion flames of fuel/oxygen mixtures, in: Proceedings of the 22nd International Symposium on Combustion, The Combustion Institute, 1988, pp. 371–388.
[20] G.H. Markstein, Correlations for smoke points and radiant emission of laminar hydrocarbon diffusion flames, in: Proceedings of the 22nd International Symposium on Combustion, The Combustion Institute, 1988, pp. 363–370.
[21] W.L. Fowler, An investigation of soot formation in axisymmetric turbulent diffusion flames at elevated pressure, in: Proceedings of the 22nd International Symposium on Combustion, The Combustion Institute, 1988, pp. 425–435.
[22] B.J. McCaffrey, M. Harkleroad, Combustion efficiency, radiation, CO and soot yield from a variety of gaseous, liquid and solid fueled buoyant diffusion flames, in: Proceedings of the 22nd International Symposium on Combustion, The Combustion Institute, 1988, pp. 1251–1261.
[23] P.H. Thomas, The size of flames from natural fires, in: Proceedings of the Ninth International Symposium on Combustion, Academic Press, New York, 1963, pp. 844–859.
[24] P.H. Thomas, Fire Spread in Wooden Cribs, Part III. The effect of Wind, Fire Research Note No. 600, Fire Research Station, Boreham Wood, England, June, 1965.
[25] G. Heskestad, Luminous heights of turbulent diffusion flames, Fire Safety J. 5 (1983) 103–108.
[26] P.K. Raj, Analysis of JP-4 Fire Test Data and Development of a Simple Fire Model, ASME Paper 81-HT-17, 20th Joint ASME-AICHE National Heat Transfer Conference, Milwaukee, August, 1981.
[27] F.P. Lees, Loss Prevention in the Process Industries, Hazard Identification, Assessment and Control, vol. 2, 2nd ed., Butterworth-Hinemann, Oxford, England, 1996.